



Turbulent Structures in Gap Flow

Ghassan Nasif^{1,2,*}, A.-M. Shinneeb², Ram Balachandar¹, Chandra Somayaji²

¹ Department of Mechanical, Automotive and Materials Engineering, University of Windsor, ON, Canada

² Mechanical Engineering Department, Higher Colleges of Technology, Abu Dhabi Men's College, Abu Dhabi, UAE

ARTICLE INFO

Article history:

Received 20 December 2021

Received in revised form 2 February 2022

Accepted 3 February 2022

Available online 24 February 2022

Keywords:

Navier-Stokes; fluid structures; open channel; gap flow; computational fluid dynamics

ABSTRACT

A computational study was carried out to investigate the effect of the gap between the body and the bed on the wake characteristics in shallow flows. A sharp-edged bluff body with two different clearances from the bed is employed in this investigation. The transient three-dimensional governing Navier-Stokes equations are numerically solved using a finite volume formulation with improved delayed detached-eddy simulation as a turbulence model. The volume of fluid approach is used in the current study as a free-surface modelling technique for locating and tracking the free surface. It is found that the existence and size of the gap influence the wake size and the location where the free surface is restored to its original and flat shape. This study also reveals that the fluid structures lose their symmetry about the center of the wake as the gap size increases.

1. Introduction

In shallow flow, the clearance between the ground and an obstacle can significantly influence the wake flow characteristics. This type of flow is often encountered in engineering applications, e.g., the airflow around solar panels, flow around vehicles, and the cooling of electronic components. Many experimental and computational studies have been carried out with sharp-edged plate, circular and square cylinders as a bluff body to investigate the influence of the gap size on the wake characteristics, such as works of Shinneeb and Balachandar [1], Shinneeb *et al.*, [2], Martinuzzi *et al.*, [3], Bosch *et al.*, [4], Essel *et al.*, [5] and Nasif *et al.*, [6, 7]. In these studies, the bluff bodies were oriented horizontally and vertically at different heights above the bed. All previous investigations agree that there is a critical gap size below which the vortex shedding is completely suppressed. On the other hand, the vortex shedding becomes independent of the size when the gap size exceeds this critical value. The fluid structures are symmetrical about the wake central plane for the case when the gap is absent. However, these fluid structures lose their regularity and two structures merge into one if the gap is introduced in a wake flow. The asymmetry and interaction between the fluid structures increase as the gap size increases [7]. A distinguished structure at the near-bed location is generated when the gap is introduced in the wake flow. The extent and strength of this structure

* Corresponding author.

E-mail address: gnasif@hct.ac.ae; nasifgg@uwindsor.ca (Ghassan Nasif)

increase with the increase of the size of the gap [7]. The interaction between this structure and the other fluid structures boosts the vertical velocity component that is normal to the bed. Yazid [8] numerically investigated the flow structure and pollutant dispersion in a 3D symmetric street canyon using a computational fluid dynamics (CFD) model. Large Eddy Simulation is used as a turbulent model in this study. It was found that as the velocity is increased, the vortex is strengthened. Different Reynolds numbers were observed to affect the turbulent structures of the pollutant inside the canyon. Generally, the leeward wall has a higher pollutant concentration as compared with the windward wall. Mustafa *et al.*, [9] presented the results of numerical simulations of vortex shedding processes at the end of a stack of parallel plates, due to an oscillating flow induced by an acoustic standing wave. In this study, the oscillating flow is simulated using Reynolds-averaged Navier-Stokes (RANS) turbulence models which are four-equation Transition SST and two-equation SST $k-\omega$. The results from this study show that the vortex shedding pattern appears more stable at all three drive ratios as the flow frequency increases

The main goal of the current study is to showcase an improved analysis in the presence of the gap in a turbulent flow. The effect of the gap size between the base of the sharp-edge bluff body and the open channel bed on the fluid structures will be investigated. These structures define the size and the wake characteristics as well as the downstream location where the free surface restores its regular shape behind the bluff body. A 3-D time-dependent simulation is carried out by numerically solving Navier-Stokes equations with improved delayed detached-eddy simulation (IDDES) as a turbulence model to obtain the results. Available data from previous experiments are used to validate the numerical results. The width of the channel in this study is broad enough so that the effect of the secondary currents is negligible at the channel central plane [10].

2. Computational Method and Validation

The current problem is simulated using STAR-CCM+ Siemens PLM commercial code with a structured mesh. First-order implicit time marching and second-order spatial differencing are used to discretize the governing equations. The volume of fluid (VoF) approach is employed in the current study as a free surface modelling technique for tracking and locating the free surface. This approach is proven to be more reliable and efficient than other methods for tackling complex free-boundary problems [11]. In the VoF method, the different fluids are assumed to share common properties at the interface(s). The solutions are attained by solving the same set of Navier-Stokes equations as in a single-phase flow for an equivalent fluid whose physical properties are calculated as functions of the physical properties of its constituent phases and their volume fractions in the control volume (cell). In the VoF method, an extra equation is required in a two-phase flow to transport the volume fraction of primary fluid [11]. In the present work, the *SST k - ω* two-equation turbulence model [12] is used as the RANS model within the IDDES simulation to model the small-scale motions. Here k is the turbulent kinetic energy and ω is the specific dissipation rate which determines the scales of turbulence. The shear stress transport (*SST*) model combines the best of two turbulent models. The use of a $k - \omega$ formulation in the inner parts of the boundary layer makes the model applicable all the way down to the wall. Therefore, this model can be used as a low Reynolds number turbulence model without any further damping functions, which are normally used with the $k - \epsilon$ model, where ϵ represents the turbulent dissipation rate. The *SST k - ω* model also switches to a $k - \epsilon$ behavior at a distance away from the wall, where the effect of the wall is less, thereby avoiding a common problem that is associated with the $k - \omega$ model. To switch between the two RANS models, Menter [13] suggested using a blending function (which involves functions of wall distance) that would include a cross-diffusion term far from the walls, but not near the walls. In the current study, various time steps

were tested to obtain a suitable time step that satisfies the local Courant-Friedrichs-Lewy (CFL) stability condition, i.e., Courant number ≤ 1.0 . [14, 15]. By definition, satisfying the CFL criterion necessitates monitoring and adjusting the time step to accomplish a balance of spatial with temporal resolution. Based on the time steps investigation, a final time step was set as 1×10^{-3} s, yielding a Courant number of less than 0.5 in the entire computational domain. Ten internal iterations were employed at each time step. In the current study, the numerical results are considered to have converged when the continuity and momentum scaled residuals fall below 10^{-6} . The mean quantities from the simulation are calculated by averaging the transient results over more than 100 vortex-shedding cycles. The temporal evolution of the transverse velocity component at a pre-defined point located three body widths downstream in horizontal planes $y/H = 0.1, 0.5,$ and 0.8 was computed with the time step for the case of no-gap. As the shed vortices travel downstream, the transverse velocity of the fluid particles downstream of the wake fluctuates about zero mean value. Knowing the time history of the waveform, the Fast Fourier Transform (FFT) is used to calculate the frequency spectra of velocity. The dominant frequency was found to be comparable at the three horizontal planes that are selected in the investigation. The vortex-shedding period (T) in this study is $T = 0.51$ s.

Figure 1 is used as the computational domain in the current study to investigate the effect of the gap on the wake flow. The Cartesian coordinate system is adopted, and the origin of the coordinate system is aligned at the central plane with the front bottom edge of the bluff body, where the X -axis represents the streamwise direction, Y -axis is the vertical location from the bottom and Z -axis is the transverse direction. The wake is generated by inserting a vertical sharp-edged plate (no. 3 in Figure 1) in a fully-developed open channel flow. A sharp-edged plate was selected to ensure that the flow separates at a fixed location along the vertical edges and to reduce the flow sensitivity to the Reynolds number. The plate is adjusted vertically at different locations to create three different gaps with the bed, i.e., $h_g/H = 0.0, 0.05,$ and 0.1 , where h_g is the gap height between the base of the plate and the bed, and H is the height of the water in the channel. The computational domain consists of two regions, comprised of water and air. All wall boundaries in contact with the water region are considered as a non-slip smooth boundary (no. 7 and lower parts of sidewalls no. 5 in Figure 1) while all sidewalls that are in contact with the air region are treated as a slip boundary. The top surface of the air region (no. 4 in Figure 1) is treated as a pressure outlet. The fully-developed turbulent flow (no. 2 in Figure 1), which is used as an inlet boundary condition at (no. 1 in Figure 1), is attained by conducting a separate simulation in an open channel without a bluff body. In the latter simulation, the velocity components and turbulent statistics are periodically mapped at the inlet from the vertical mid-plane at $X/L=0.5$ until reaching a fully-developed velocity profile. Here, L is the length of the channel. A pressure outlet is used as a boundary condition at the outlet of the channel (no. 6 in Figure 1).

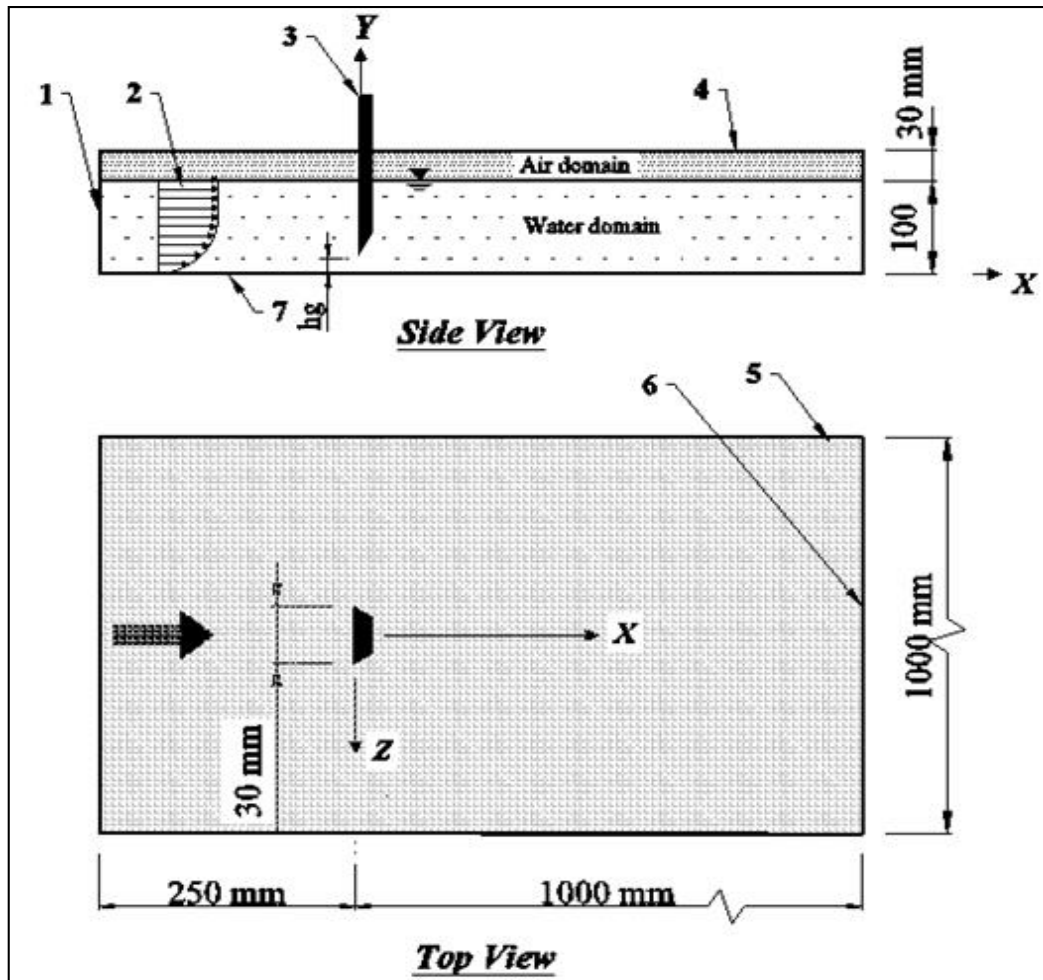


Fig. 1. Model setup with relevant boundary conditions

Cell sensitive study is carried out in this study to evaluate the final cell count. The criterion for choosing the final cell count is based on the requirement that the half-width of the wake $z_{0.5}$ does not change significantly by increasing the number of cells [7, 16]. The non-dimensional frequency, i.e., Strouhal number (St), of the vortex shedding and the drag coefficient (C_d) of the bluff body are also evaluated and compared for all the grids that are used in the sensitivity study. Based on the cell independent study, the final cell count which is employed to discretize the flow domain shown in Figure 1 is 20×10^6 structured elements. Normalized cell sizes based on the height of the water in the open channel range between $5.5 \times 10^{-4} - 4.2 \times 10^{-2}$. The cells are clustered in the gap and along the water-air interface to reduce the numerical dissipation that is associated with the VoF model. A fine resolution of prism layers is employed near the wall. The non-dimensional wall-normal distance is $y^+ < 3.0$, therefore the first layer of the prism layer is located in the viscous sub-layer region. The prism layers next to the wall act as a bridge to cross from the wall boundary to the fluid region. More information to evaluate the size of the prism layer can be found in our previous study [17, 18].

Validations are carried out with a no-gap case by comparing the numerical results from the simulations, i.e., mean and statistical features with available data from previous PIV experiments reported in Refs. [19, 20]. Figure 2 shows selected samples of the validation process that employ mean quantities of the flow field. In this figure, the normalized stream-wise velocity U/U_∞ and transverse velocity W/U_∞ from computation are compared with the experimental data at the wake region, where U , W , and U_∞ is the streamwise, transverse and free stream velocity of the flow in the channel, respectively. These data are extracted at locations $Y/H = 0.5$ and $X/H = 0.5$ and plotted versus

the normalized transverse direction Z/H as shown in Figure 2. To assess the performance of the turbulence model, a RANS-based Reynolds Stress Model (RSM) was also used in the validation process to evaluate the turbulence characteristics of the wake. The computational results from the RSM model are compared with the results obtained from the Detached Eddy Simulation model and experimental data to select a suitable turbulence model. The conclusion that can be extracted from the validation process (not all results are presented here for brevity) is that the DES model predicts and can reproduce the experimental data better than the RSM model, and therefore employed as a turbulence model in this study

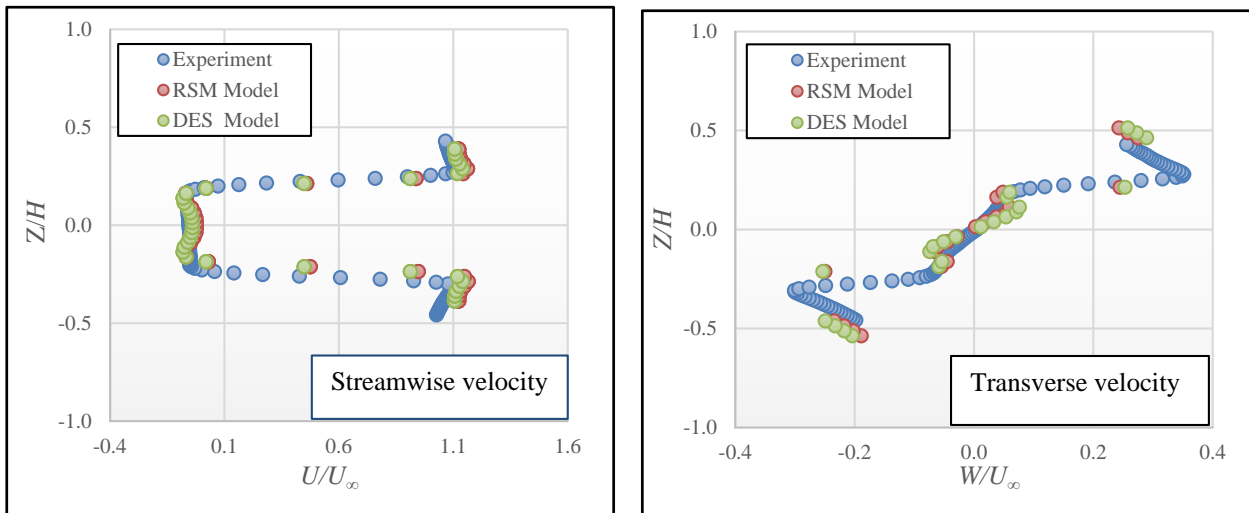


Fig. 2. Validation carried out at $Y/H = 0.5$, $Z/H = 0.5$

3. Results and Discussion

The effect of the gap size is apparent in the shallow wake flow as shown in Figure 3. In this figure, the mean velocity vector superimposed by a contour of normalized streamwise vorticity ($\omega_x B/U_\infty$) is extracted at the downstream location of $X/H = 4.0$ from the bluff body for all three cases that have been used in the study, where ω_x , B and U_∞ represent the streamwise vorticity component, bluff body width, and the free stream velocity, respectively. Various fluid structures can be distinguished in Figure 3. The mechanism of generation and dynamics of these structures were discussed in our previous study [7].

The four fluid patterns marked with letters A, B, C, and D in Figure 3a are symmetrical about the wake central plane for the case of $h_g/H = 0.0$. However, these structures lose their symmetry or two patterns merge into one pattern as gap introduced in the flow as shown in Figure 3b and 3c. The distortion degree of the fluid patterns depends on the gap size. The horseshoe vortex is evident in Figure 3a and marked with the letter (A). The formation of the horseshoe vortex is attributed to the interaction between the non-uniform approaching velocity (boundary layer), front of the bluff body, and the bed of the channel. The variation in the stagnation pressure along the front face of the bluff body will act to generate a horseshoe vortex tube near the channel bed. This tube stretches downstream along the sides of the body as a necklace structure. The horseshoe structure attenuates as the gap is introduced in the wake flow. The residuals of the horseshoe vortex become unorganized and merge with the structure (B) as shown in Figures 3b and 3c (structure AB) due to the increase of the sideways entrainment process to the wake region. The structure (B) resides near the channel bed and has the same sense of angular motion as the horseshoe legs. The mechanism of formation and

development of structure (B) can be comprehended from the instantaneous flow analysis and its formation is elaborated in [7]. The extent of the maximum magnitude of the streamwise vorticity contours marked with letter (C) in Figure 3 expands in the spanwise and vertical directions as the gap clearance increases. This is attributed to the enhancement of the vertical velocity component, which increases as the gap size increases. The vertical velocity impinges the free surface and diverts outwards from the wake central plane and acts to expand the contour of streamwise vorticity.

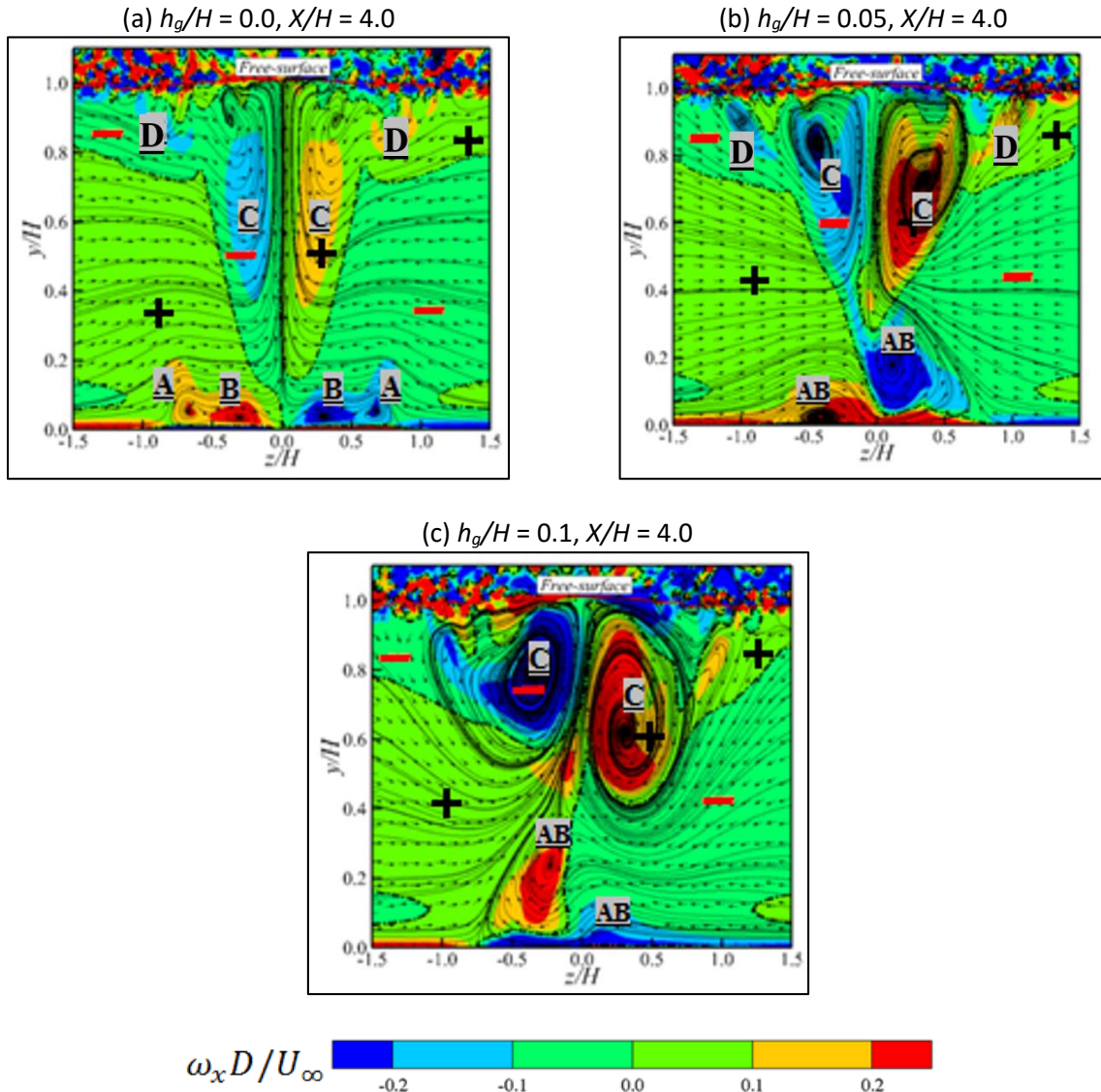
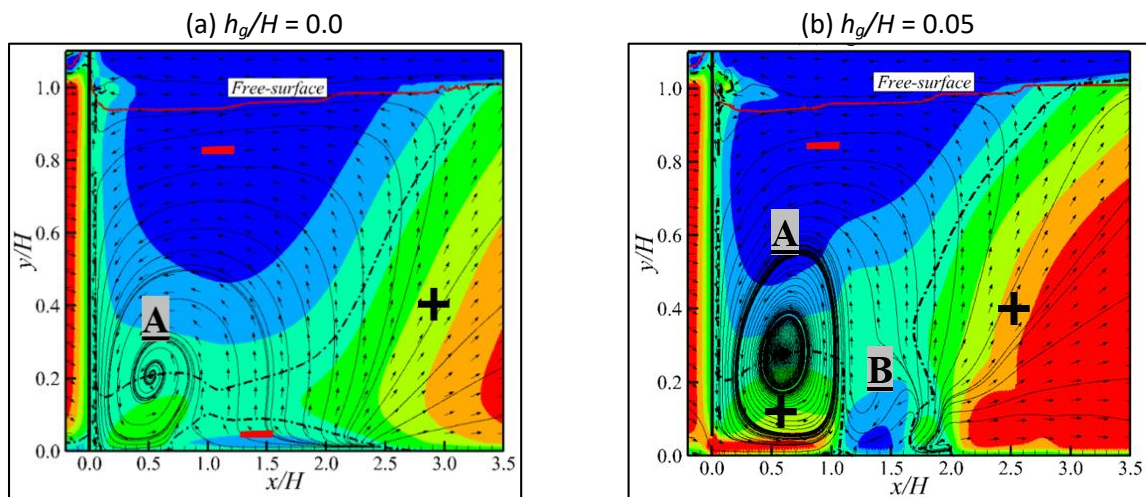


Fig. 3. Mean velocity vector superimposed by a contour of streamwise vorticity ($\omega_x B / U_\infty$)

More insight into the gap flow characteristics can be obtained by extracting the streamwise velocity profiles at the channel central plane for the three cases employed in the study as shown in Figure 4. The thick red solid line in Figure 4, labeled as the *free surface* at location $y/H \approx 1.0$, represents the interface between the two fluids, i.e., water and air, while the thick black dash-dotted line presents the zero streamwise velocity contour lines. Across this line the streamwise velocity switches between positive and negative. A unique feature of shallow wakes flow is the three-dimensional roll-up structure between the bed and the free surface. This structure, which is marked with the letter (A) has been observed immediately behind the bluff body in all three cases of Figure 4. This conclusion agrees with the investigation of Akilli and Rockwell [21], and Nasif *et al.*, [22]. The

presence of a three-dimensional roll-up structure in all three cases of this study indicates that the presence of the gap does not affect the generation of this structure. However, the interaction between the flow through the gap and this structure changes the characteristics of the three-dimensional roll-up structure from the usual spiral shape shown in Figure 4a to a bubble shape as shown in Figures 4b and c. Additionally, this structure lifts away from the bed by a distance comparable to the gap clearance as the flow through the gap forces this structure away from the bed as shown in Figure 4b and 4c. Another observation that can be drawn from Figure 4 is that the extent of the recirculation (negative) flow zone in Figure 4 decreases while the size of the positive velocity region increases with the increase of the gap size. This is ascribed to two contrasting effects: on the one hand, the flow from the gap appears to be entirely swallowed by the recirculation zone. This will transfer the kinetic energy of the gap flow to the recirculation region. On the other hand, the spread and expansion of the lower flow associated with the larger gap size act to reduce the adverse pressure gradient (positive gradient) in the wake region and finally decreases the size of the recirculating zone. The latter observation is agreed with the experimental investigations carried out by Essel *et al.*, [5]. One of the consequences of the gap in the wake flow is the development of a distinct structure marked with the letter (B) in Figures 4b and 4c. The generation of this structure is mostly ascribed to the extension of the contour of the maximum positive velocity and withdrawing the contour of the maximum negative velocity towards the bluff body. This structure is missing in Figure 4a due to the absence of the gap. The structure (B) plays a significant role in returning the free surface of the water to its original flat shape (at $Y/H = 1.0$) at a shorter downstream location from the bluff body. The free surface returns to its flat shape earlier as the gap size increases (see Figures 4b and 4c). The interaction between the structures (A) and (B) acts to enhance the vertical component velocity and drive more fluid towards the free surface as the gap size increases.



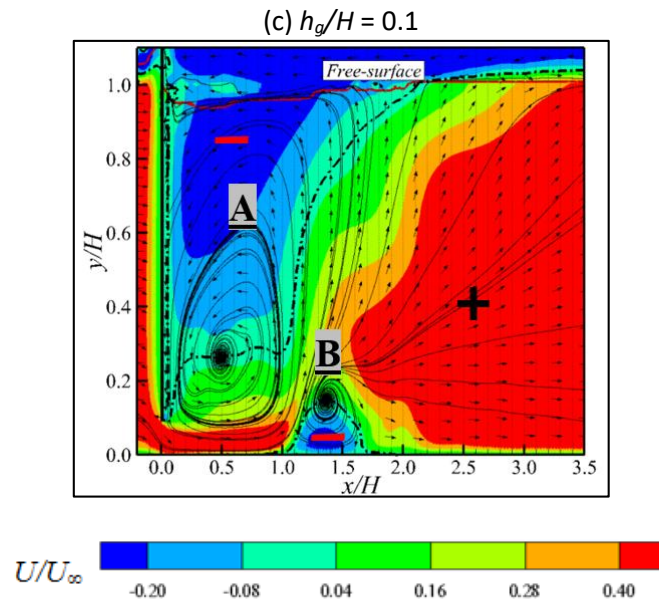


Fig. 4. Averaged velocity vector at the vertical plane $z/H = 0.0$, overlapped by contours of the mean streamwise velocity U/U_∞

Figure 5 shows the three-dimensional fluid structures in the mean flow for the three cases used in the investigation. These structures are colored by the normalized streamwise vorticity ($\omega_x B/U_\infty$). The horseshoe vortex (A) generates in the front face of the bluff body and spans downstream into the wake region. This structure appears in Figure 5a and also is captured in Figure 3a. Another structure (B) appears in Figure 5a at the downstream location $X/H > 2.0$ (captured in Figure 3a as B). This structure has two parallel components of counter-rotating tubes, generates near the legs of the horseshoe structure. One of the features of shallow-wake flows is the presence of the streamwise vorticity tubes, near the free surface [7, 23]. This structure marked with letter (E) in Figure 5a (D in Figure 3a) acts to thrust the fluid chunks from the wake core to the surrounding region. The formation of this structure beneath the free surface is attributed to the impingement of moving fluid particles through the wake central plane with the free surface. Another structure is observed in Figure 5a marked with the letter (D). This structure represents the averaging of the transient recirculation zone behind the bluff body. This structure absorbs the kinetic energy from the outer flow to overcome the bed shear stress and endures its location behind the bluff body. Downstream from the bluff body, the flow of the surrounding start decelerating and the energy that is used to sustain this structure is not enough to cope with the bed shear stress. Therefore, the interaction between this structure and the bed declines. This is the location where structure (D) starts to separate from the bed and align with the mean flow, generating structure (C) (structure C in Figure 3a). It is clearly shown in Figure 3a and 5a that structure (C) occupies a larger region and has an opposite direction of rotation compared to structures (A) and (B). The effect of the gap on the fluid structures is evident in Figure 5b and 5c where only small traces of the horseshoe structure (A) appear in Figures 5b and 5c. The degree of attenuation and distortion in the horseshoe structure depends on the gap size. It is clearly shown in Figure 5c that the horseshoe vortex is almost disappeared with the gap size of $h_g/H = 0.1$. Another observation that can be drawn from Figures 5b and 5c, is that the region of the recirculation flow, represented by structure (D), is shrunk as the gap size increases. This is attributed to that gap flow will sustain the wake region with energy and therefore increases the momentum and reduces the volume of this region. The effect of the gap on structure (C) is obvious in Figures 5b and 5c. The X-vorticity component of these structures increases with the gap size. This structure also approaches the free surface as the gap height increases to $h_g/H = 0.1$ as shown in Figs 3c and 5c. The enhanced

vertical velocity component acts to drive this structure towards the free surface. This structure enlarges and distorts as the gap clearance increases.

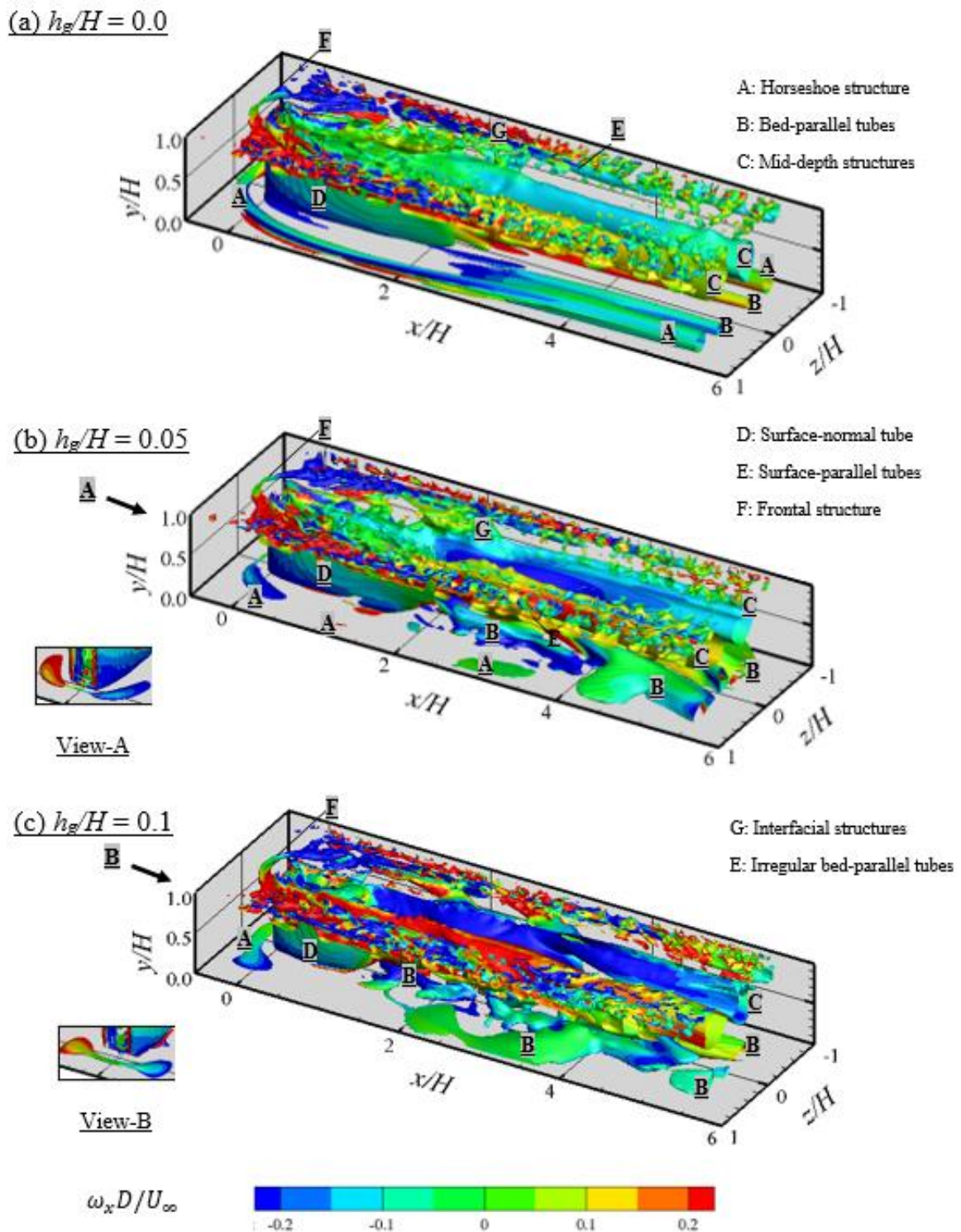


Fig. 5. Fluid structures in the mean flow for all cases that used in the investigation; (a) $h_g/H = 0.0$, (b) $h_g/H = 0.05$ and (c) $h_g/H = 0.1$. "This figure is reproduced from ref. [7] with the permission of AIP Publishing"

4. Conclusions

The current computational investigation is aimed to examine the effect of the gap in the wake flow. Two gap sizes were employed in this study to evaluate the effect of gap size on the flow characteristics and different fluid structures. The numerical study was achieved by using the finite volume method. A volume of fluid model is used to capture the free surface at the water-air interface. The computational results are validated by a referenced no-gap case. The following results are concluded from the current study:

- i. The fluid structures are symmetrical about the wake central plane in the absence of a gap. However, as the gap is introduced in the wake flow, the fluid structures lose their symmetry. The degree of asymmetry and interaction of different fluid structures increases with the gap size.
- ii. A distinct structure at the near-bed location appears when the gap is present in the wake flow. The size and vorticity magnitude of this structure depend on the gap size. This structure plays a significant role in returning the free surface of the water to its original flat shape at a shorter downstream location from the bluff body due to the enhancement of the vertical velocity components of the fluid near the bed of the channel.
- iii. One of the effects of the gap in the wake flow is to minimize the volume of the wake behind the bluff body. This is attributed to that gap flow will sustain the wake region with energy and therefore increases the momentum and reduces the volume of this region.
- iv. At the center of the wake, the size of the negative velocity contour shrinks while the size of the positive velocity contour increases with the increase of the gap size.
- v. The three-dimensional roll-up structure is a signature of the shallow wake flow. This structure is also captured when the gap is present in the shallow flow. However, the roll-up structure is switched from its usual spiral pattern to a bubble pattern when the gap is introduced to the flow.

Acknowledgment

This research was made possible by the facilities of the Shared Hierarchical Academic Computing Network and Compute/Calcul Canada

References

- [1] Shinneeb, A-M., and R. Balachandar. "Effect of gap flow on the shallow wake of a sharp-edged bluff body—turbulence parameters." *Journal of Turbulence* 17, no. 1 (2016): 122-155. <https://doi.org/10.1016/j.jasrep.2016.05.067><https://doi.org/10.1080/14685248.2015.1088156>
- [2] Shinneeb, A-M., R. Balachandar, and K. Zouhri. "Effect of gap flow on the shallow wake of a sharp-edged bluff body—Coherent structures." *Physics of Fluids* 30, no. 6 (2018): 065107. <https://doi.org/10.1063/1.5022252>
- [3] Martinuzzi, R. J., and M. AbuOmar. "Study of the flow around surface-mounted pyramids." *Experiments in fluids* 34, no. 3 (2003): 379-389. <https://doi.org/10.1007/s00348-003-0594-0>
- [4] Bosch, G., M. Kappler, and W. Rodi. "Experiments on the flow past a square cylinder placed near a wall." *Experimental thermal and fluid science* 13, no. 3 (1996): 292-305. [https://doi.org/10.1016/S0894-1777\(96\)00087-8](https://doi.org/10.1016/S0894-1777(96)00087-8)
- [5] Essel, Ebenezer E., Mark F. Tachie, and Ram Balachandar. "Time-resolved wake dynamics of finite wall-mounted circular cylinders submerged in a turbulent boundary layer." *Journal of Fluid Mechanics* 917 (2021). <https://doi.org/10.1017/jfm.2021.265>

- [6] Nasif, G., R. Balachandar, and R. M. Barron. "Mean characteristics of fluid structures in shallow-wake flows." *International Journal of Multiphase Flow* 82 (2016): 74-85. <https://doi.org/10.1016/j.ijmultiphaseflow.2016.03.001>
- [7] Nasif, G., R. Balachandar, and R. M. Barron. "Influence of bed proximity on the three-dimensional characteristics of the wake of a sharp-edged bluff body." *Physics of Fluids* 31, no. 2 (2019): 025116. <https://doi.org/10.1063/1.5085666>
- [8] Yazid, MNA Mohd. "Large Eddy Simulations of Pollutant Dispersion in a Street Canyon." *Journal of Advanced Research in Fluid Mechanics and Thermal Sciences* 8, no. 1 (2015): 11-19.
- [9] Mustaffa, Siti Hajar Adni, Fatimah Al Zahrah Mohd Saat, and Ernie Mattokit. "Turbulent Vortex Shedding across Internal Structure in Thermoacoustic Oscillatory Flow." *Journal of Advanced Research in Fluid Mechanics and Thermal Sciences* 46, no. 1 (2018): 175-184.
- [10] Shinneeb, A-M., G. Nasif, and R. Balachandar. "Effect of the aspect ratio on the velocity field of a straight open-channel flow." *Physics of Fluids* 33, no. 8 (2021): 085110. <https://doi.org/10.1063/5.0057343>
- [11] Nichols, B. D., C. W. Hirt, and R. S. Hotchkiss. "Volume of fluid (VOF) method for the dynamics of free boundaries." *J. Comput. Phys* 39 (1981): 201-225. [https://doi.org/10.1016/0021-9991\(81\)90145-5](https://doi.org/10.1016/0021-9991(81)90145-5)
- [12] Menter, Florian R. "Two-equation eddy-viscosity turbulence models for engineering applications." *AIAA journal* 32, no. 8 (1994): 1598-1605. <https://doi.org/10.2514/3.12149>
- [13] Menter, F. R., and M. Kuntz. "Adaptation of eddy-viscosity turbulence models to unsteady separated flow behind vehicles." In *The aerodynamics of heavy vehicles: trucks, buses, and trains*, pp. 339-352. Springer, Berlin, Heidelberg, 2004. https://doi.org/10.1007/978-3-540-44419-0_30
- [14] Spalart, Philippe R., and Craig Streett. *Young-person's guide to detached-eddy simulation grids*. No. NAS 1.26: 211032. 2001.
- [15] Spalart, Philippe R. "Detached-eddy simulation." *Annual review of fluid mechanics* 41 (2009): 181-202. <https://doi.org/10.1146/annurev.fluid.010908.165130>
- [16] Nasif, G., R. Balachandar, and R. M. Barron. "Supercritical flow characteristics in smooth open channels with different aspect ratios." *Physics of Fluids* 32, no. 10 (2020): 105102. <https://doi.org/10.1063/5.0021609>
- [17] Nasif, Ghassan Gus. "CFD Simulation of Oil Jets with Application to Piston Cooling." (2014).
- [18] Nasif, G., R. M. Barron, and R. Balachandar. "Numerical simulation of piston cooling with oil jet impingement." *Journal of Heat Transfer* 138, no. 12 (2016). <https://doi.org/10.1115/1.4034162>
- [19] Singha, A. "Shallow Wake in Open Channel Flow—Look into the Vertical Variability (Ph. D. dissertation)." *Department of Mechanical, Automotive and Materials Engineering, University of Windsor, Canada* (2009).
- [20] Heidari, Mehdi, Ram Balachandar, Vesselina Roussinova, and Ronald M. Barron. "Characteristics of flow past a slender, emergent cylinder in shallow open channels." *Physics of Fluids* 29, no. 6 (2017): 065111. <https://doi.org/10.1063/1.4986563>
- [21] Akilli, H. Ü. S. E. Y. İ. N., and D. O. N. A. L. D. Rockwell. "Vortex formation from a cylinder in shallow water." *Physics of Fluids* 14, no. 9 (2002): 2957-2967. <https://doi.org/10.1063/1.1483307>
- [22] Nasif, G., R. Balachandar, and R. M. Barron. "Characteristics of flow structures in the wake of a bed-mounted bluff body in shallow open channels." *Journal of Fluids Engineering* 137, no. 10 (2015). <https://doi.org/10.1115/1.4030537>
- [23] Maheo, P. "Free Surface Turbulent Shear Flow (Ph. D. dissertation)." *California Institute of Technology, CA, USA* (1999).